

Limits to photosynthesis: seasonal shifts in supply and demand for CO₂ in Scots pine

Zsofia R. Stangl¹ , Lasse Tarvainen² , Göran Wallin²  and John D. Marshall¹ 

¹Department of Forest Ecology and Management, Swedish University of Agricultural Sciences, SE-901 83 Umeå, Sweden; ²Department of Biological and Environmental Sciences, University of Gothenburg, SE-413 19 Gothenburg, Sweden

Authors for correspondence:

John D. Marshall

Email: john.marshall@slu.se

Zsofia R. Stangl

Email: zsofia.reka.stangl@slu.se

Received: 25 August 2021

Accepted: 2 November 2021

New Phytologist (2022) 233: 1108–1120

doi: 10.1111/nph.17856

Key words: boreal forest, carboxylation capacity, diffusional limitations, light limitation, mesophyll conductance, *Pinus sylvestris*, stomatal conductance, temperature limitation.

Summary

- Boreal forests undergo a strong seasonal photosynthetic cycle; however, the underlying processes remain incompletely characterized. Here, we present a novel analysis of the seasonal diffusional and biochemical limits to photosynthesis (A_{net}) relative to temperature and light limitations in high-latitude mature *Pinus sylvestris*, including a high-resolution analysis of the seasonality of mesophyll conductance (g_m) and its effect on the estimation of carboxylation capacity ($V_{C_{\text{max}}}$).
- We used a custom-built gas-exchange system coupled to a carbon isotope analyser to obtain continuous measurements for the estimation of the relevant shoot gas-exchange parameters and quantified the biochemical and diffusional controls alongside the environmental controls over A_{net} .
- The seasonality of A_{net} was strongly dependent on $V_{C_{\text{max}}}$ and the diffusional limitations. Stomatal limitation was low in spring and autumn but increased to 31% in June. By contrast, mesophyll limitation was nearly constant (19%). We found that $V_{C_{\text{max}}}$ limited A_{net} in the spring, whereas daily temperatures and the gradual reduction of light availability limited A_{net} in the autumn, despite relatively high $V_{C_{\text{max}}}$.
- We describe for the first time the role of mesophyll conductance in connection with seasonal trends in net photosynthesis of *P. sylvestris*, revealing a strong coordination between g_m and A_{net} , but not between g_m and stomatal conductance.

Introduction

Terrestrial biosphere models (TBMs) typically use the Farquhar, von Caemmerer, and Berry (FvCB) model (Farquhar *et al.*, 1980) to predict photosynthetic carbon (C) assimilation by C₃ plants, including responses to rising temperatures and atmospheric CO₂. Now 40 yr old, the FvCB model has been developed and improved over time. Initially, it defined C assimilation rate as determined by the more limiting of two biochemical processes: carboxylation capacity of Rubisco ($V_{C_{\text{max}}}$) and the capacity of ribulose 1,5-bisphosphate (RuBP) regeneration by electron transport. A third biochemical process, the capacity for triose phosphate utilization (Sharkey, 1985), was identified and incorporated into the model later. Nevertheless, under current ambient CO₂ concentrations, light-saturated photosynthesis is considered primarily Rubisco-limited (Sage & Kubien, 2007). Therefore, TBMs commonly represent photosynthetic capacity in terms of $V_{C_{\text{max}}}$.

Light availability and temperature are the most important environmental factors determining the seasonality of biochemical capacity and net photosynthesis (A_{net}) in the boreal region, whereas soil water content is often considered nonlimiting (Bergh *et al.*, 1998). Changing seasonal light conditions determine the rate of photosynthesis as well as the length of the growing season (Hari &

Mäkelä, 2003; Fracheboud *et al.*, 2009; Bauerle *et al.*, 2012; Hall *et al.*, 2013). In the boreal region, the effect on A_{net} is strongest in the autumn when days get shorter and low irradiance suppresses A_{net} (Bergh *et al.*, 1998; Hari & Mäkelä, 2003; Mäkelä *et al.*, 2004; Hall *et al.*, 2013; Tarvainen *et al.*, 2015). In the spring, days are already long by the time it is warm enough for photosynthetic activity and bud burst (Bergh *et al.*, 1998). To model the seasonality of photosynthesis in *Pinus sylvestris*, Mäkelä *et al.* (2004) defined a photosynthetic capacity term that changes over the season in correlation with temperature and highlighted temperature as a strong driver of C uptake in boreal conifers (Bergh *et al.*, 1998; Hari & Mäkelä, 2003; Mäkelä *et al.*, 2004; Jensen *et al.*, 2015). Warming experiments have confirmed this key role of temperature by showing that increasing the ambient temperature extended the photosynthetic season due to early induction of photosynthetic activity in the spring (Wallin *et al.*, 2013), and by maintaining high photosynthesis rates in the autumn at latitudes where light conditions are more favourable (Stinziano *et al.*, 2015; Richardson *et al.*, 2018). However, the effect of warming on the seasonal maximum rates of photosynthesis is unclear and is likely to change with the magnitude of the warming and to differ across species based on their acclimation strategy (Hall *et al.*, 2013; Kurepin *et al.*, 2018; Lamba *et al.*, 2018; Dusenge *et al.*, 2020).

The FvCB model estimates biochemical capacity and A_{net} based on the CO_2 concentration inside the chloroplasts (C_c). C_c has traditionally been assumed equal to the intercellular CO_2 concentration (C_i) based on the assumption of negligible resistance to CO_2 diffusion between the intercellular space and the chloroplast. C_i is determined by the diffusional resistance of the stomata and is readily calculated from gas-exchange measurements, with the resistance typically represented by its inverse, stomatal conductance (g_s). Although it is now accepted that C_c is not equal to C_i and that leaf internal conductance, referred to as mesophyll conductance (g_m), has substantial influence on CO_2 diffusion (Flexas *et al.*, 2008; Warren, 2008), C_i is still commonly used in the FvCB model because estimating C_c is technically challenging (Pons *et al.*, 2009; Stangl *et al.*, 2019). This approach, however, overestimates the CO_2 concentration in the chloroplast and yields an estimate of ‘apparent’ biochemical capacity that is lower than the actual capacity (Sun *et al.*, 2014b). This distinction between apparent and actual capacity does not matter if apparent $V_{C_{\text{max}}}$ is treated as an empirical parameter (Medlyn *et al.*, 2002a,b). However, combining biochemical and diffusional processes into apparent capacity restricts the possibility to account for their divergent responses to the environment and can lead to misinterpretations of the underlying reasons for changes in photosynthetic activity (Sun *et al.*, 2014a; Xu *et al.*, 2020).

Owing to the resistance of the stomata and the mesophyll to CO_2 diffusion, C_c is typically between 150 and 250 $\mu\text{mol mol}^{-1}$ under current ambient CO_2 concentrations. Therefore, a change in g_s and/or g_m will often change C_c along the steepest part of the photosynthetic CO_2 -response curve, thereby producing a relatively large effect on the rate of CO_2 uptake (Fig. 1a). Stomata operate under active regulatory control in an effort to balance the C gain with water (H_2O) loss (Cowan & Farquhar, 1977; Ball *et al.*, 1987; Leuning, 1995). Consequently, g_s is correlated with the rate of photosynthesis, the rate of transpiration, and the evaporative demand (vapour pressure deficit, VPD) of the ambient air (Katul *et al.*, 2009; Medlyn *et al.*, 2011). Mesophyll conductance and C_c remain difficult to measure in the field; therefore, data on the response of g_m to different environmental parameters under natural conditions is limited (Flexas, 2016; Rogers *et al.*, 2017; Dewar *et al.*, 2018; Stangl *et al.*, 2019; Schiestl-Aalto *et al.*, 2021). Nevertheless, it has received substantial interest because an increase in mesophyll conductance could enhance C uptake without increasing H_2O loss in the process (Flexas *et al.*, 2013; Flexas, 2016), thus having a substantial impact on water-use efficiency (WUE) (Stangl *et al.*, 2019; Ma *et al.*, 2021). Owing to this role, g_m is considered a ‘central player’ in acclimation and adaptation of plants to a future with warmer and drier climates (Warren, 2008; Flexas *et al.*, 2012; Flexas, 2016).

Several methods have been used to evaluate the effect of diffusional constraints on photosynthesis, but the differential method and the gas-phase elimination method (Farquhar & Sharkey, 1982; Jones, 1985) are the most common. The differential method considers the ratio between the slope of the supply function (proportional to g) and the slope of the demand function (proportional to biochemical capacity) at the point where they intersect; that is, the operating point, which is given by A_{net} and

C_i or C_c (Jones, 1985; Grassi & Magnani, 2005; Xu *et al.*, 2019). However, this method requires knowledge of the full photosynthetic CO_2 -response curve, as the estimation of the biochemical capacity is based on the derivative of the curve at the operating point. To analyse the limitation seasonally requires seasonal estimates of CO_2 -response curves under changing leaf phenology and variable environmental conditions, thereby introducing additional assumptions and uncertainty.

By contrast, the gas-phase elimination method evaluates the diffusional limitations due to stomatal conductance L_{g_s} and mesophyll conductance L_{g_m} , relative to the potential rate of photosynthesis A_{C_a} if the CO_2 concentration in the chloroplasts were equal to the ambient CO_2 concentration C (Fig. 1a; Farquhar & Sharkey, 1982; Bernacchi *et al.*, 2002). Assuming that $V_{C_{\text{max}}}$ is the main limiting biochemical process at CO_2 concentrations below C_a , the biochemical demand for CO_2 can be represented by $V_{C_{\text{max}}}$, and it can be used to calculate A_{C_a} . On the other hand, g_s and g_m represent the supply of CO_2 to the site of carboxylation inside the chloroplast. Given constant g_s and g_m , the ratio of A_{net} to A_{C_a} is smaller and the diffusional limitation is greater when $V_{C_{\text{max}}}$ is high and the initial slope of the A_{net}/C_c curve is steep, compared with when $V_{C_{\text{max}}}$ is small and the initial slope of the A_{net}/C_c curve is relatively flat (Fig. 1b). This method highlights the changing significance of CO_2 supply with varying CO_2 demand. The differential and the elimination methods generated similar results (29.7% and 27.7% limitation, respectively) when analysing photosynthetic g_s limitations in Norway spruce (Wallin *et al.*, 1992), but the second method is more straightforward to interpret and requires fewer assumptions.

We conducted continuous measurements of shoot-scale gas exchange and online C isotope discrimination under natural conditions throughout a whole growing season in a mature stand of the boreal conifer *P. sylvestris*. Continuous measurements of A_{net} , g_s , and g_m from early April to late October allowed us, first, to describe the seasonality of stomatal and mesophyll conductance and evaluate the coordination between the two conductances on a seasonal scale; second, to quantify the ratio between ‘apparent’ and ‘actual’ $V_{C_{\text{max}}}$; third, to analyse the seasonality of $V_{C_{\text{max}}}$ and diffusional limitations of A_{net} ; and fourth, to describe the seasonality of temperature and photosynthetic photon flux density (PPFD) controls over A_{net} .

Materials and Methods

Site description

The study was conducted on mature (*c.* 100-yr-old) *P. sylvestris* (Scots pine) trees at the Rosinedalsheden experimental forest in northern Sweden (64°10'N, 19°45'E). The experiment was established in 2005, in a naturally regenerated, even-aged stand, and consists of a control site and a site with intensive nitrogen (N) fertilization. A more detailed description of the experiment can be found in Lim *et al.* (2015). The current study was conducted on the control site, from the beginning of April to the end of October in 2017, covering the photosynthetic season typical for the area and the species. The year 2017 was relatively cold for

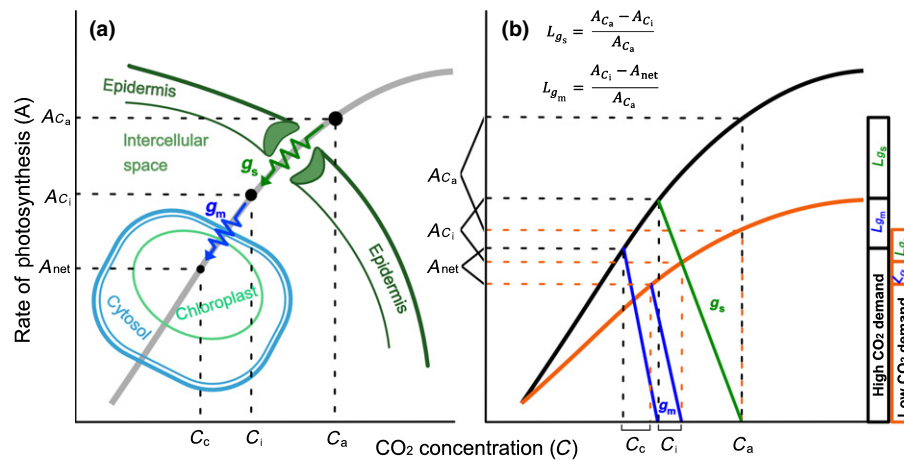


Fig. 1 Conceptual figure showing the relationship between the demand for, and the supply of, CO₂ on the rate of photosynthesis. (a) The biochemical capacity represents the demand for CO₂, and determines the shape of the CO₂-response curve (grey line). Along that curve, stomatal and mesophyll conductance (g_s and g_m) determine the supply of CO₂ and affect the reduction of CO₂ concentration from the atmosphere (C_a) to the intercellular space (C_i) and the site of carboxylation inside the chloroplast (C_c). (b) Considering constant g_s (slope of green line) and g_m (slope of blue lines), when the demand for CO₂ is high (black response curve) the ratio between observed and potential rate of photosynthesis is higher than when demand is low (orange response curve). Accordingly, the proportional limitation of photosynthesis due to g_s and g_m (L_{g_s} and L_{g_m}) is higher when the demand for CO₂ is high compared to when it is low, as depicted by the bars on the right. The equations show the relationship between the rate of photosynthesis and L_{g_s} and L_{g_m} , where A_{net} is the actual rate of photosynthesis, and A_{c_i} and A_{c_a} are the potential rates without L_{g_m} and without L_{g_m} and L_{g_s} respectively.

the area, with a mean temperature of $7.8 \pm 4.7^\circ\text{C}$ (mean \pm SD) for the period of April to October, which was on average $1.2 \pm 0.7^\circ\text{C}$ (mean \pm SD) lower than the average of the same period in the preceding 10 yr according to data by the Swedish Meteorological and Hydrological Institute.

Gas-exchange and online $\delta^{13}\text{C}$ measurements

A custom-built multichannel gas-exchange system (Wallin *et al.*, 2001; Tarvainen *et al.*, 2016) was coupled to a G2131-i cavity ring-down spectrophotometer (CRDS; Picarro Inc., Santa Clara, CA, USA) to continuously measure shoot-scale CO₂ and H₂O exchange and photosynthetic ¹³C discrimination. A detailed description of the method and the set-up can be found in Stangl *et al.* (2019). Briefly, four temperature-controlled shoot cuvettes made of transparent Plexiglas, equipped with a sensor for PFD, were secured onto a 1-yr-old upper canopy shoot on four individual trees. To avoid condensation within the cuvettes and downstream tubing, the humidity of incoming air was controlled by a cold trap (3°C below ambient), so that it did not exceed *c.* 85%. Furthermore, cuvette temperatures were kept on average 0.2°C above the ambient and the tubing was insulated and heated (Hall *et al.*, 2009). The partial pressures of CO₂ and H₂O vapour in the air flow of sample (i.e. cuvette) and reference (i.e. ambient air) channels were measured in parallel using CIRAS-1 differential infrared gas analysers (IRGAs; PP Systems, Hitchin, UK). The CRDS was connected in line with the IRGA sample channel. The system cycled through four cuvette and two noncuvette reference lines at 7 min intervals, resulting on average in one measurement of each cuvette per hour and two measurements of ambient air per hour. The IRGAs were calibrated with 400 μmol mol⁻¹ CO₂ gas and with a dew-point generator (LI-610; Li-Cor, Lincoln, NE, USA) at the beginning and at the end of the

growing season. Additionally, every hour the IRGAs were zero calibrated and the system ran a cross-calibration protocol to match values in the sample and reference channels. The CRDS was manually calibrated once per week using two reference gases with known CO₂ concentrations (411 μmol mol⁻¹, SD = 5.1; 1606 μmol mol⁻¹, SD = 13.1) and $\delta^{13}\text{C}$ values (-32.36‰, SD = 0.09; -4.14‰, SD = 0.06). In addition, the $\delta^{13}\text{C}$ values were corrected for the sensitivity of the CRDS to CO₂ and H₂O vapour concentration (Stangl *et al.*, 2019). Photosynthesis caused the CO₂ concentration inside the cuvettes to drop below the CO₂ concentration of ambient air. The magnitude of the draw-down was controlled by the flow rate through the cuvette and was adjusted over the course of the season to ensure sufficient drawdown for accurate measurement of the CO₂, H₂O, and CO₂ isotope fluxes (more details are given in the Results section).

Data analysis

The measurements and data presented in this paper cover the photosynthetic season of *P. sylvestris* at the latitude of the site, from 1 April (week 14) to 31 October (week 44). Photosynthetic rates were calculated daily between 05:00 h and 20:00 h (GMT + 1), and this data set was used to fit weekly light-response models. For all further analysis, midday data between 09:00 h and 14:00 h were considered (i.e. $n = 5$ data points measured during 5 h), because this was when the rate of photosynthesis reached its daily peak across the whole season. The cuvette-based median of these measurements was taken to represent the daily maximum rate of photosynthesis for the individual shoots. Owing to technical problems, 36% of the data points were filtered out. ¹³C discrimination was not measured during weeks 29 and 30. The data are presented on a weekly basis, and most weeks (22 out of 31) have $n = 4$ replicates (i.e. trees). Because of the data filtering, 4 wk have

$n = 3$ and 5 wk have $n = 2$. Individual weeks included a minimum of 6, a maximum of 28, and an average of 18.9 data points. The STATS package (v.4.0.0) of R (v.3.3.2) was used for statistical analysis and curve fitting. All variability is given as standard error, unless stated otherwise. All data is provided in Supporting Information Dataset S1.

Leaf gas-exchange parameters

Net photosynthesis (A_{net}), stomatal conductance (g_s), and the intercellular CO_2 concentration (C_i) were calculated from the gas-exchange data according to von Caemmerer & Farquhar (1981). Mesophyll conductance (g_m) was estimated from ^{13}C discrimination, assuming that the daytime mitochondrial respiration (R_m) (Methods S1) was isotopically disconnected from the Calvin–Benson–Bassham cycle, as proposed by Busch *et al.* (2020):

$$g_m = \frac{1 + t}{1 - t} \frac{A_{\text{net}} \left(b - a_m - \frac{R_m}{A_{\text{net}}} \frac{\alpha_b}{\alpha_c \alpha_R} e \right)}{C_a (\Delta_i - \Delta_o)} \quad \text{Eqn 1}$$

In Eqn 1, t is a ternary correction factor (Methods S2; Farquhar & Cernusak, 2012), and b , a_m , and e are the $^{12}\text{C}/^{13}\text{C}$ fractionation during carboxylation (29‰), dissolution and diffusion through H_2O (1.8‰), and mitochondrial respiration, respectively. R_m and e were estimated as previously described in Stangl *et al.* (2019; Methods S1, S2), assuming a 40% reduction of respiration in the light (Way & Yamori, 2014) and recent photosynthate as respiratory substrate (Wingate *et al.*, 2007; Gessler *et al.*, 2008; Farquhar & Cernusak, 2012). The reference values for R_m were estimated from night-time respiration during the darkest hour of the night (23:00 h–00:00 h) and the corresponding cuvette temperatures, on a weekly basis (Methods S1). For all calculations, we considered the CO_2 concentration inside the shoot cuvette as C_a . Δ_i is the discrimination when assuming infinite g_m and accounting for respiratory and photorespiratory fractionation (Methods S2; Busch *et al.*, 2020), and Δ_o is the observed discrimination estimated from the $\delta^{13}\text{C}$ measured with the CRDS, as described in Stangl *et al.* (2019; Methods S2). α_b and α_c are the isotope effects of carboxylation and mitochondrial respiration, respectively, and α_R is given according to Busch *et al.* (2020):

$$\alpha_R = 1 + \frac{R_m}{A_{\text{net}}} \frac{e}{\alpha_c} \quad \text{Eqn 2}$$

Estimates of g_m were compared with the g_m values produced by the traditional model (Farquhar & Cernusak, 2012; Evans & von Caemmerer, 2013). Although 69.5% of the estimates were within a 5% similarity range, we found that the model proposed by Busch *et al.* (2020) produced less variable g_m estimates, especially when A_{net} and the concentration difference between ambient and cuvette CO_2 were low. We considered A_{net} as too low when it was below $1 \mu\text{mol CO}_2 \text{ m}^{-2} \text{ s}^{-1}$ and the CO_2 concentration difference as too low when it fell below $9 \mu\text{mol mol}^{-1}$. The

latter contrasts with the $20 \mu\text{mol mol}^{-1}$ limit suggested by Pons *et al.* (2009) and applied in our previous study (Stangl *et al.*, 2019). These looser constraints allowed us to extend our analysis into April and October.

The CO_2 concentration at the site of carboxylation (C_c) was calculated from g_m using the following relationship:

$$C_c = C_i - \frac{A_{\text{net}}}{g_m} \quad \text{Eqn 3}$$

In all calculations, boundary-layer resistance was neglected, because boundary-layer conductance has previously been found to be high due to the fans in our cuvettes (Uddling & Wallin, 2012). Projected leaf area was estimated at the end of the measurement campaign by collecting and scanning the needles from the shoots enclosed in the cuvettes. The scanned images were analysed using WINSEEDLE PRO 5.1a (Regent Instruments, Quebec, QC, Canada).

Light-saturated rates of photosynthesis

To identify light-saturated rates of photosynthesis, light-response curves (LRCs) were fitted to A_{net} vs PPFd on a weekly basis, using the nonrectangular hyperbolic model by Marshall & Biscoe (1980):

$$A_{\text{net}} + R_d = \frac{m \text{PPFD} (A_{G_{\text{max}}} - \theta A_{\text{net}})}{(1 - \theta) m \text{PPFD} + (A_{G_{\text{max}}} - \theta A_{\text{net}})} \quad \text{Eqn 4}$$

which on expansion gives

$$\theta A_{\text{net}}^2 - (A_{G_{\text{max}}} + m \text{PPFD} - \theta R_d) A_{\text{net}} + m \text{PPFD} [A_{G_{\text{max}}} - (1 - \theta) R_d] - R_d A_{G_{\text{max}}} = 0 \quad \text{Eqn 5}$$

m , the initial slope of the LRC; θ , the degree of curvature; $A_{G_{\text{max}}}$, maximum rate of gross photosynthesis; PPFd units are $\mu\text{mol m}^{-2} \text{ s}^{-1}$. The LRCs were fitted in two steps. First, a linear regression model was fitted to A_{net} vs PPFd for all PPFd $< 50 \mu\text{mol m}^{-2} \text{ s}^{-1}$ to determine the rate of CO_2 release in the dark (R_d) and the initial slope of the response curve (m). Second, to determine $A_{G_{\text{max}}}$ and θ , the model described in Eqn 5 was fitted to the whole range of A_{net} vs PPFd using the nls() function in the R STATS package and the values of R_d and m as determined in the first step. Some examples of fitted LRCs are shown in Fig. S1(a).

The maximum rate of net photosynthesis was calculated for each week of the season as:

$$A_{\text{max}} = A_{G_{\text{max}}} - (1 - \theta) R_d \quad \text{Eqn 6}$$

The spatial distance between the light sensor and the cuvette (*c.* 5 cm apart) caused scattering in the LRC, exemplified by few high A_{net} data points at low PPFd and low A_{net} data points at high PPFd (Fig. S1b). To avoid this technical bias, we used A_{net} , rather than PPFd, to identify light-saturated rates of photosynthesis and considered all measurement points light-saturated

where A_{net} was equal to or higher than 90% of A_{max} , so that the limit of light-saturated rates was:

$$A_{\text{sat}} = 0.9 \times A_{\text{max}} \quad \text{Eqn 7}$$

Temperature optimum of photosynthesis

To avoid the confounding effect of light, we used only light-saturated rates of A_{net} to analyse the temperature response of photosynthesis across the season. We fitted temperature-response curves to all observed light-saturated A_{net} and corresponding cuvette temperature (T_{cuv}) during April, May, mid-season (June and July), and late season (August–October) separately (Fig. S2a–d). In April, A_{net} was not responsive to temperature (Fig. S2a). During the rest of the season the optimum temperature shifted slightly from 17.5°C in May to 19°C in June–July and 23°C August–October, with A_{net} at optimum temperature changing from $10.2 \pm 0.2 \mu\text{mol m}^{-2} \text{s}^{-1}$ to $18.5 \pm 0.2 \mu\text{mol m}^{-2} \text{s}^{-1}$ and to $14.4 \pm 0.2 \mu\text{mol m}^{-2} \text{s}^{-1}$, respectively. We defined a range around the thermal optimum where the slope was $< 0.2 \mu\text{mol m}^{-2} \text{s}^{-1} \text{ } ^\circ\text{C}^{-1}$ and A_{net} was still within the range of the standard error of the maximum rates (Fig. S3). In May, this range was 15–20°C, in June–July it was 18–20°C, and in August–October it was 20–26°C. Because 20°C was always in this range, we used it as the season-long optimum of A_{net} . The fitted temperature-response models were then used to estimate A_{20} , the rate of photosynthesis at optimum temperature for each period.

Biochemical capacity of photosynthesis

We assumed that under light-saturated conditions, the biochemical capacity for photosynthesis is equal to the carboxylation capacity of Rubisco ($V_{C_{\text{max}}}$). $V_{C_{\text{max}}}$ was estimated from light-saturated A_{net} using the one-point method (Wilson *et al.*, 2000; De Kauwe *et al.*, 2016), as

$$V_{C_{\text{max}}} = (A_{\text{net}} + R_d) \left(\frac{C + K_m}{C - \Gamma^*} \right) \quad \text{Eqn 8}$$

$C = C_i$ in the case of $V_{C_{\text{max}}}(C_i)$ and C_c in the case of $V_{C_{\text{max}}}(C_c)$; Γ^* , C compensation point derived from the specificity of Rubisco to C, and calculated according to Bernacchi *et al.* (2001) for $V_{C_{\text{max}}}(C_i)$ and according to Bernacchi *et al.* (2002) for $V_{C_{\text{max}}}(C_c)$; K_m is given by:

$$K_m = K_C \left(1 + \frac{O}{K_O} \right) \quad \text{Eqn 9}$$

O , partial pressure of oxygen (O_2) in the chloroplast ($210 \text{ mmol mol}^{-1}$); K_C and K_O , the Michaelis–Menten constants of CO_2 and O_2 , respectively. K_C and K_O were estimated from the temperature-response functions proposed by Bernacchi *et al.* (2001) for $V_{C_{\text{max}}}(C_i)$ and Bernacchi *et al.* (2002) for $V_{C_{\text{max}}}(C_c)$.

To compare carboxylation capacity in different parts of the season, we estimated $V_{C_{\text{max}}}$ at a common temperature of 25°C. We fitted published temperature-response functions to May,

mid-season (June and July), and late-season (August–October) data (Fig. S4). In agreement with previous studies in another conifer species (Jensen *et al.*, 2015), $V_{C_{\text{max}}}$ in April was constant and not responsive to temperature (Fig. S4a,e); therefore, we present the mean value of the data points in that month. $V_{C_{\text{max}}}(C_i)$ was fitted with the temperature-response function published by Tarvainen *et al.* (2018), which was established from A/C_i response curves measured at different temperatures on the same trees in August 2013. We also used these full response curves to alleviate concern over our use of the one-point method (Burnett *et al.*, 2019); the values obtained by both methods were similar.

$V_{C_{\text{max}}}(C_c)$ was fitted with the temperature-response function proposed by Bernacchi *et al.* (2001), because this function does not require any assumption about the thermal optimum, for which we did not have sufficient data. In both cases, the reference value at 25°C (k_{25}), was allowed to vary to find the best fit for the data while all other model parameters were held constant.

Mechanistic limitations of A_{net}

The diffusional limitations were estimated relative to the potential rate of photosynthesis without diffusional limitations (i.e. infinite g_m and infinite g_s) (Farquhar & Sharkey, 1982). The potential rate of photosynthesis without mesophyll limitation (A_{C_i}) was calculated from $V_{C_{\text{max}}}(C_c)$ and Eqn 7 by assuming $C_c = C_i$, and the potential rate of photosynthesis without any diffusional limitation (A_{C_a}) was calculated by assuming $C_c = C_a$. The relative contributions of stomatal limitation and mesophyll limitation to the reduction of photosynthesis were then evaluated relative to A_{C_a} and estimated using Eqn 10 and Eqn 11, respectively:

$$L_{g_s} = \frac{A_{C_a} - A_{C_i}}{A_{C_a}} \quad \text{Eqn 10}$$

$$L_{g_m} = \frac{A_{C_i} - A_{\text{net}}}{A_{C_a}} \quad \text{Eqn 11}$$

These limitations were estimated for each gas-exchange measurement for which $V_{C_{\text{max}}}$ and the conductances were available (i.e. light-saturated rates).

Empirical limitations of A_{net}

In a separate, parallel analysis, we assessed limitations due to PPF and temperature. This was done by comparing the observed rate of photosynthesis with a reference photosynthetic rate. For these analyses, the reference rate was not A_{C_a} as earlier herein, but instead was an empirical maximum related to saturating light intensity (A_{sat}) and optimum temperature (A_{20}), respectively. Light limitations were evaluated on all data. Temperature limitations were evaluated on light-saturated photosynthesis data to avoid the confounding effect of light limitation, and the light-saturated values were determined as described earlier. The PPF limitation was expressed as:

$$L_{\text{PPFD}} = \frac{A_{\text{sat}} - A_{\text{net}}}{A_{\text{sat}}} \quad \text{Eqn 12}$$

The temperature limitation was expressed as:

$$L_T = \frac{A_{20} - A_{net}}{A_{20}} \quad \text{Eqn 13}$$

Note that $L \leq 0$ means that $A_{net} \geq A_{sat}$ or A_{20} , respectively, which we define as no limitation.

This second analysis does not account separately for the diffusion and $V_{C_{max}}$ limitations, but instead includes them within the empirically fitted temperature and PPFD limitations. Note that this analysis evaluates the ‘daily’ effect of temperature on the observed A_{net} , rather than the seasonal changes in photosynthetic capacity. For clarity the effect of temperature on the seasonality of photosynthetic capacity will from now on be termed the ‘seasonal’ temperature effect.

Results

Seasonality of midday gas-exchange parameters

CO₂ concentrations were measured or inferred from the atmosphere to the chloroplast throughout the photosynthetic season. Atmospheric CO₂ concentration fell from 410 μmol mol⁻¹ in the spring to 380 μmol mol⁻¹ at the peak of the summer and then rose again to c. 410 μmol mol⁻¹ during autumn. The drawdown between atmospheric and cuvette CO₂ concentration varied between 9 and 93 μmol mol⁻¹ during midday photosynthesis, causing cuvette CO₂ concentration to drop, on average, to 310 μmol mol⁻¹ during peak photosynthetic activity, from mid-June to late August (Fig. 2a). This large drawdown improved the precision of our estimates of isotopic fractionation. During this period, the mean C_i was 234 ± 2 μmol mol⁻¹, and the mean C_c was 177 ± 2 μmol mol⁻¹, with the lowest value at 103 μmol mol⁻¹, still well above the photosynthetic CO₂ compensation point (Γ^*) estimated for the same period (30 ± 3 μmol mol⁻¹). The mean drawdown between C_a and C_i was 99 ± 2 μmol mol⁻¹, and the mean drawdown between C_i and C_c was 59 ± 2 μmol mol⁻¹.

These concentration declines were driven by seasonal changes in gas-exchange characteristics. Midday A_{net} peaked, on average, at 15.8 ± 0.3 μmol CO₂ m⁻² s⁻¹ at the end of June–beginning of July, with maximum rates as high as 20.4 μmol CO₂ m⁻² s⁻¹ (Fig. 2b), and gradually declined after the summer solstice (21 June). By early August, mean rates of A_{net} had dropped to 10.7 ± 0.2 μmol CO₂ m⁻² s⁻¹. Midday stomatal conductance reached its seasonal maximum at the same time as A_{net} , at 0.170 ± 0.006 mol CO₂ m⁻² s⁻¹ bar⁻¹, but stayed high well into September (Fig. 2b). Mesophyll conductance followed the seasonality of A_{net} closely and peaked at mean midday values of 0.28 ± 0.014 mol CO₂ m⁻² s⁻¹ bar⁻¹ (Fig. 2b). The mean ratio of the conductances (g_s/g_m) under light-saturated conditions was 0.88 ± 0.08 , and the median was 0.60 (Fig. S5). High g_s/g_m was observed in the beginning (2.2 ± 0.28) and end of the season (0.89 ± 0.33), and the lowest ratio was observed in June (0.53 ± 0.08). The correlation between g_s/g_m and the week number was significant ($P < 0.001$), meaning that the ratio varied over the season.

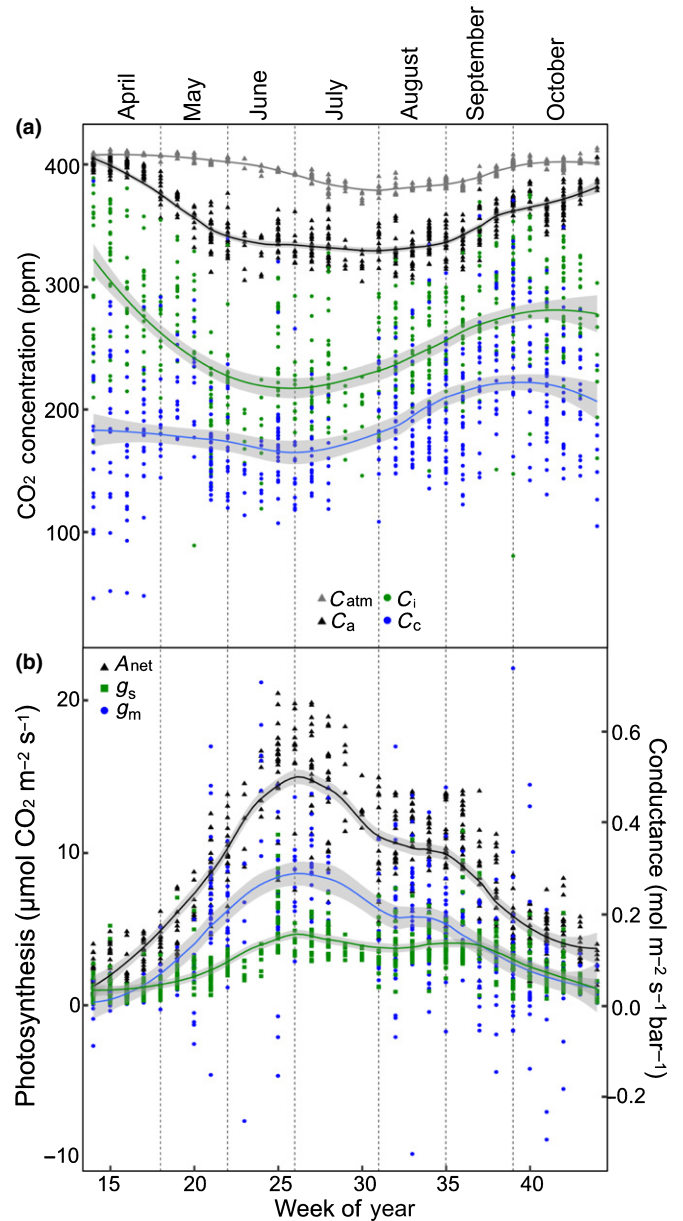


Fig. 2 Seasonality of atmospheric CO₂ concentration at the site, and internal CO₂ concentrations, photosynthesis, and stomatal and mesophyll conductance in upper canopy shoots of *Pinus sylvestris*. (a) The carbon concentration in the atmosphere (grey), inside the shoot cuvettes (black), in the intercellular space (C_i , green), and in the chloroplast (C_c , blue). (b) Net photosynthesis (A_{net} , black), stomatal conductance (g_s , green), and mesophyll conductance (g_m , blue). In both panels, the symbols represent the daily median midday values of each shoot, and the solid lines represent the weekly mean with the grey shading representing SE around the mean, as estimated by loess fit.

Seasonal biochemical capacity of photosynthesis

We used the one-point method to estimate $V_{C_{max}}$ at ambient temperature from all light-saturated values of A_{net} based either on C_i or C_c . The two $V_{C_{max}}$ estimates were similar except at the peak of the photosynthetic season; between weeks 23 and 27, when carboxylation capacity was highest, $V_{C_{max}}(C_c)$ (actual) was on

average 14% higher than $V_{C_{\max}}(C_i)$ (apparent) (Figs 3, S6). The seasonality of both $V_{C_{\max}}$ estimates under ambient temperature conditions followed the pronounced seasonality of A_{net} , with much higher values in June and July and lowest values earlier and later in the season (Fig. 3).

We fitted published temperature response functions (Bernacchi *et al.*, 2001; Tarvainen *et al.*, 2018) to the data to estimate $V_{C_{\max}}(C_i)$ and $V_{C_{\max}}(C_c)$ at a common temperature of 25°C (Table 1; Fig. S2). Carboxylation capacity at 25°C was highest during June and July: $V_{C_{\max}}(C_i) = 129 \pm 5 \mu\text{mol m}^{-2} \text{s}^{-1}$, and $V_{C_{\max}}(C_c) = 147 \pm 4 \mu\text{mol m}^{-2} \text{s}^{-1}$ (Table 1); and it was 30–33% lower in late season and 45–50% lower in May (Table 1). In April, carboxylation capacity was only about 5% of the value during the peak of the season, and it was constant across all temperatures (Fig. S4a,b): $V_{C_{\max}}(C_i) = 6.2 \pm 0.8 \mu\text{mol m}^{-2} \text{s}^{-1}$, and $V_{C_{\max}}(C_c) = 4.7 \pm 0.5 \mu\text{mol m}^{-2} \text{s}^{-1}$ (Table 1).

Diffusional limitations of light-saturated photosynthesis

Diffusional limitations of light-saturated A_{net} due to stomatal and mesophyll conductance showed different seasonal patterns. Stomatal limitation (L_{g_s}) had a significant seasonality ($P < 0.001$), with a maximum of $31 \pm 8\%$ in June and lower values at the beginning ($7.9 \pm 1.1\%$) and end of the season ($8.7 \pm 3.4\%$) and a mean of $21 \pm 4\%$ (Fig. 4). By contrast, mesophyll limitation

Table 1 Carboxylation capacity of Rubisco at 25°C (k_{25}), and the r^2 and P values of the model fitted to the data.

	k_{25}	r^2	P	Model
$V_{C_{\max}}(C_i)^a$				
April	4.7 ± 0.5	0.18	0.004	Tarvainen <i>et al.</i> (2018)
May	70 ± 3	0.71	< 0.001	
June + July	129 ± 5	0.52	< 0.001	
August–October	93 ± 3	0.79	< 0.001	
$V_{C_{\max}}(C_c)^a$				
April	6.2 ± 0.8	0.09	0.047	Bernacchi <i>et al.</i> (2001)
May	73 ± 2	0.64	< 0.001	
June + July	147 ± 4	0.72	< 0.001	
August–October	105 ± 2	0.89	< 0.001	

^aMaximum carboxylation capacity calculated from the CO_2 concentration in the intercellular space ($V_{C_{\max}}(C_i)$) and in the chloroplast ($V_{C_{\max}}(C_c)$).

(L_{g_m}) was relatively stable over the season, with a mean of $19 \pm 1\%$ and no significant seasonality ($P = 0.64$, Fig. 4). The seasonal means of L_{g_s} and L_{g_m} were similar. However, during the peak of photosynthetic activity in June and July, the relative reduction of A_{C_a} due to L_{g_s} was significantly higher than due to L_{g_m} ($P <$

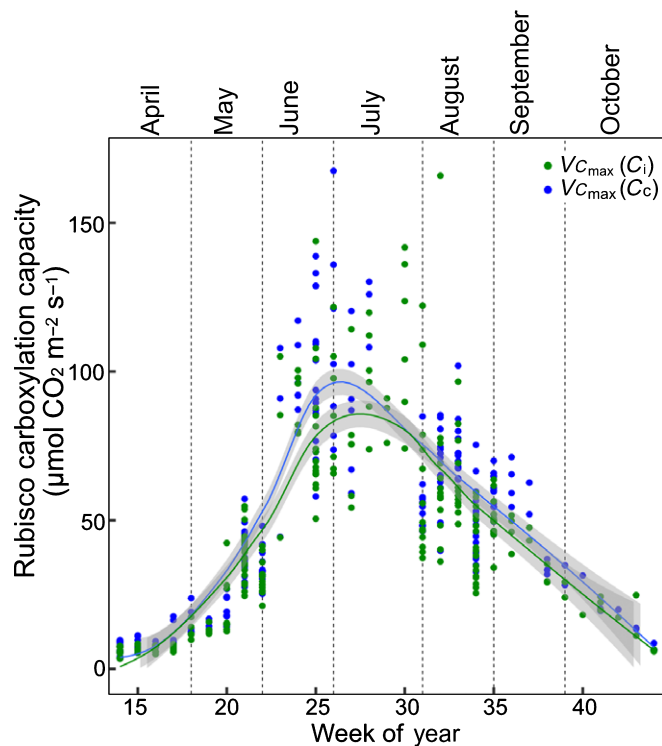


Fig. 3 Seasonality of carboxylation capacity of *Pinus sylvestris* at ambient temperature. Maximum carboxylation capacity estimated based on the CO_2 concentration in the intercellular space ($V_{C_{\max}}(C_i)$, green) and in the chloroplast ($V_{C_{\max}}(C_c)$, blue). The symbols represent the daily median midday values of each shoot, and the solid lines represent the weekly mean with the grey shading representing SE around the mean, as estimated by loess fit.

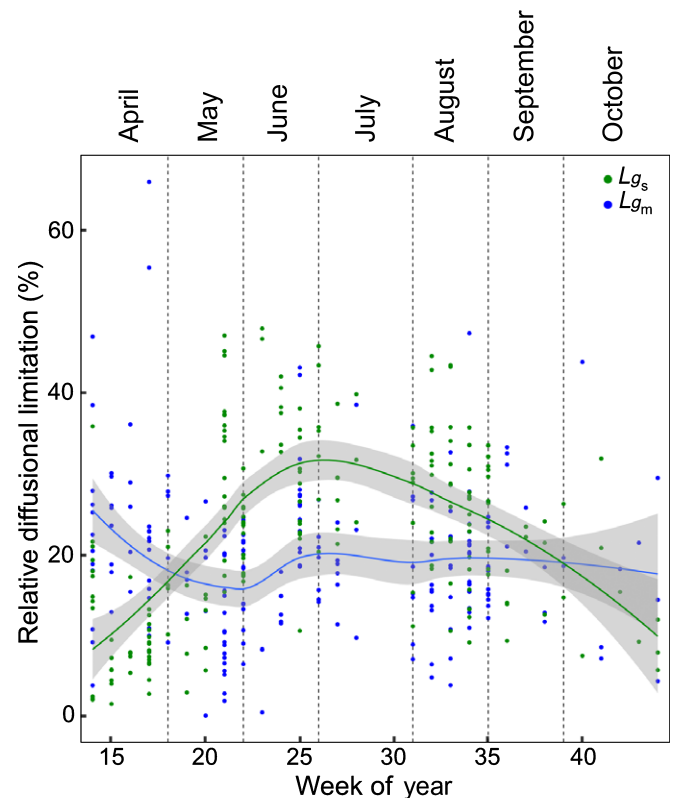


Fig. 4 Stomatal and mesophyll limitations (L_{g_s} and L_{g_m}) were similar in magnitude over the season but showed different seasonal patterns in *Pinus sylvestris*. The seasonality of the relative limitation of light-saturated photosynthesis by stomatal conductance (L_{g_s} , green) and mesophyll conductance (L_{g_m} , blue). The symbols represent the mean daily midday values of each shoot, and the solid lines represent the weekly mean, with the grey shading representing SE around the mean, as estimated by loess fit.

0.001), and together they reduced A_{net} to about 50% of its potential rate.

Environmental limitations of photosynthesis: light and temperature

Our empirical analysis of daily limitations on A_{net} due to daily light and temperature assigned all variation in A_{net} to the light and temperature conditions on the day in question. We found that these fast-acting light and temperature limitations were strongest late in the season, when $V_{C_{\text{max}}}$ remained relatively high. The daily limitations were weak in the early season, when $V_{C_{\text{max}}}$ was strongly reduced due to incomplete recovery. Nevertheless, even during the long days of the early and mid-season, in most weeks > 50% of midday data were collected under nonsaturating light conditions (Fig. 5a), and average midday A_{net} was $12 \pm 1.9\%$ below the light-saturated values of photosynthesis (Fig. 5b). Light limitation further increased from the summer solstice (week 25) onward, reaching $39 \pm 2.6\%$ in October, reducing midday A_{net} almost to 60% of A_{sat} estimated for the same period (Fig. 5b). Light-saturated A_{net} was not limited by temperature until the end of August. From September onward, daily L_T increased sharply to > 50% by the end of October (Fig. 5b).

Discussion

Using high-resolution continuous measurements of gas exchange and C isotope discrimination, we present for the first time the seasonality of mesophyll conductance, and $V_{C_{\text{max}}}$ estimates corrected for mesophyll conductance, together with photosynthesis and stomatal conductance in mature *P. sylvestris* under natural conditions. The rate and seasonality of A_{net} agreed well with previously reported observations in *P. sylvestris* at similar latitudes and under similar climatic conditions (Troeng & Linder, 1982; Mäkelä *et al.*, 2004; Kolari *et al.*, 2014; Yang *et al.*, 2020). Notably, a strong decline of A_{net} was observed in August, which could indicate a resource reallocation to the newly developed shoots, which are fully expanded by the end of July. The seasonal pattern of g_m was similar to that of A_{net} , in that both peaked during June and July and gradually declined thereafter. This confirms previous reports of coordination between A_{net} and g_m (Dewar *et al.*, 2018; Stangl *et al.*, 2019; Knauer *et al.*, 2020) and shows that it was maintained despite seasonal changes in environment and phenology.

In contrast to A_{net} and g_m , g_s remained high until early September, even during the warmest days in July. Water availability has traditionally been considered nonlimiting in the boreal region (Bergh *et al.*, 1998). However, some more recent analysis suggested that year-to-year variation in precipitation (Lim *et al.*, 2015) and a drought-related increase of VPD (Tian *et al.*, 2021) can influence the productivity of boreal *P. sylvestris*, at least on sandy soils. Either way, the consistently high midday g_s observed in our measurements suggests that the trees were not under H₂O stress during the study period. The lack of coordination between g_m and g_s is also noteworthy, particularly in light of a recent report to the contrary, which was based on point measurements across several plant species (Ma *et al.*, 2021).

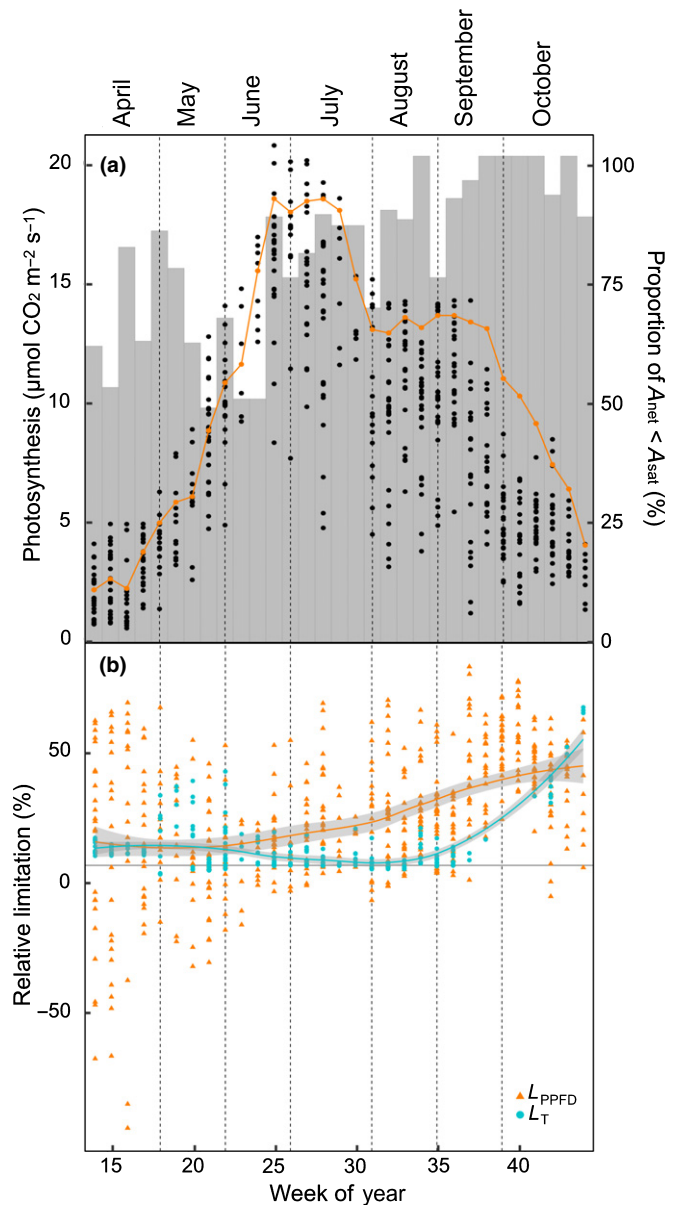


Fig. 5 Limiting light conditions were frequent over the entire season, whereas temperature was most limiting late in the season for midday photosynthesis. (a) The daily midday mean rates of net photosynthesis (A_{net} , black symbols), the lowest light-saturated values of net photosynthesis (A_{sat} , orange), and the weekly proportion of nonsaturated to light-saturated rates of A_{net} (grey bars) in the upper canopy shoots of *Pinus sylvestris*. (b) The relative limitations of A_{net} by light (L_{PPFD} , orange; PPFD, photosynthetic photon flux density) and the relative limitation of light-saturated A_{net} by temperature (L_T , blue). The symbols represent the mean daily midday values of each shoot, and the solid lines represent the weekly mean, with the grey shading representing SE around the mean, as estimated by loess fit.

The modelling of mesophyll conductance is an important issue because g_m serves as a linkage between the C isotopic composition of plant tissues and photosynthetic gas exchange, including WUE (Stangl *et al.*, 2019; Gimeno *et al.*, 2021; Ma *et al.*, 2021; Schiestl-Aalto *et al.*, 2021). The adjustment is necessary because isotopic composition is determined in the chloroplast, whereas

H₂O vapour evaporates from the intercellular space through the stomata and this path-length difference must be accounted for by incorporating the g_s/g_m term into the calculations. The seasonal mean of g_s/g_m (0.88 ± 0.08) in our analysis was within the range of the mean reported by Ma *et al.* (2021). However, owing to the strong seasonality of g_s/g_m , its median was 0.60 (Fig. S5). Choosing either of the two values to represent seasonal g_s/g_m would result in a 10–15% difference in the estimated WUE according to the sensitivity analysis by Ma *et al.* (2021). This argues against the use of a constant g_s/g_m in *P. sylvestris* on a seasonal scale and raises questions about the generality of this parameterization. Given that our data instead suggest that mesophyll limitation is nearly constant, and that the seasonality of g_m is strongly coordinated with that of A_{net} , these results can provide an alternative means of modelling mesophyll conductance. It would be worthwhile to test these alternative models against the range of conditions from top to bottom of the canopy. We have described such a model in a recent paper, but there we assumed that g_m does not change vertically within the crown (Schiestl-Aalto *et al.*, 2021). We hope to explore the incorporation of seasonal variation and the assumption of constant mesophyll limitation in future modelling work (Schiestl-Aalto *et al.*, 2021). To do so here would be beyond the scope of the current study.

We focused our attention on Rubisco capacity because we assumed that carboxylation of RuBP was the biochemical process determining the potential rate of A_{net} across the season (Yang *et al.*, 2020). We used the one-point method (Wilson *et al.*, 2000) to estimate $V_{C_{max}}$ from light-saturated values of A_{net} . The generality of this method has previously been tested in a meta-analysis across 564 species (De Kauwe *et al.*, 2016), but questions about it have been raised (Burnett *et al.*, 2019). The one-point method is based on the assumption that light-saturated photosynthesis is primarily Rubisco limited under current ambient CO₂ concentrations. Recently Busch & Sage (2017) proposed that the C_c at which Rubisco limitation switches to limitation by electron transport capacity is temperature dependent, and can be as low as 120 $\mu\text{mol mol}^{-1} \text{CO}_2$ at 15°C to *c.* 250 $\mu\text{mol mol}^{-1} \text{CO}_2$ at 25°C. According to their analysis in sweet potato plants, photosynthesis in our trees would only be Rubisco limited during the warmest days in the middle of the season and would be limited by electron transport capacity on most days, or triose phosphate utilization on very cold days. In this case, the one-point method would estimate an apparent biochemical capacity rather than actual $V_{C_{max}}$ (Wilson *et al.*, 2000). At the same time, their analysis does not take the seasonality of $V_{C_{max}}$ into account, which alters the dynamics between different biochemical limitations (Yang *et al.*, 2020). Our estimates of $V_{C_{max}}(C_i)$ at 25°C in August ($93 \pm 3 \mu\text{mol m}^{-2} \text{s}^{-1}$, Table 1) agreed well with estimates based on A/C_i response curves on the very same trees and during August 2013 ($94 \pm 9 \mu\text{mol m}^{-2} \text{s}^{-1}$, Tarvainen *et al.*, 2018). Furthermore, previously published temperature-response functions of $V_{C_{max}}$ in these trees (Tarvainen *et al.*, 2018) described our $V_{C_{max}}(C_i)$ estimates well from May to October and across a wide range of temperatures (Table 1; Fig. S4b–d). These results support the applicability of the one-point method for our data set. In addition, our seasonal estimates of $V_{C_{max}}(C_i)$ agreed well with

previously published values in *P. sylvestris* at similar latitudes (Kolari *et al.*, 2014; Yang *et al.*, 2020) and other conifers in both boreal and more temperate climates (Han *et al.*, 2004; Jensen *et al.*, 2015). Most importantly, these studies reported similarly pronounced reduction of $V_{C_{max}}$ in early spring, which could not be detected when $V_{C_{max}}$ was measured within a shorter seasonal timeframe (Jach & Ceulemans, 2000; Medlyn *et al.*, 2002a,b; Miyazawa & Kikuzawa, 2006).

The difference between $V_{C_{max}}(C_i)$ and $V_{C_{max}}(C_c)$ was, on average, 14% at the peak of the photosynthetic season (Table 1), and it was not significant in the early and late season. This is substantially lower than the > 50% difference previously reported for oak and ash (Grassi & Magnani, 2005) but is higher than that found in hybrid poplar clones (Xu *et al.*, 2020). The wide range of these results suggests a strong interspecific variation in the relationship between Rubisco capacity and g_m . At the same time, the methods used to estimate g_m were also quite different in the different studies, which may have affected estimates of C_c as well (Pons *et al.*, 2009). During most of the season, our results agree well with the previously reported strong similarity between $V_{C_{max}}(C_i)$ and $V_{C_{max}}(C_c)$ from a range of evergreen tropical and temperate species (Bahar *et al.*, 2018). Nevertheless, that study found some deviation from the 1 : 1 correlation in species with high carboxylation capacity. Similarly, we report a significant difference between $V_{C_{max}}(C_c)$ and $V_{C_{max}}(C_i)$ during the middle of the season for the higher values of carboxylation capacity (Figs 3, S6). The relevance of these environmental responses of $V_{C_{max}}$ and g_m for global-scale modelling is still debated (Medlyn *et al.*, 2002a,b; Sun *et al.*, 2014a,b; Rogers *et al.*, 2017). However, their importance is without doubt when the properties of g_m , or individual enzymes, are to be studied (Xu *et al.*, 2020). For example, the decline of $V_{C_{max}}(C_i)$ at high temperature is often attributed to the declining stability of Rubisco activase (Sage *et al.*, 2008), whereas it could in fact be an effect of reduced g_m (Xu *et al.*, 2020). Disentangling these responses is important for understanding their drivers and predicting the acclimation capacity of different species, or engineering plants that are more productive and resilient under future conditions (Flexas, 2016).

We used the stomatal and mesophyll conductance data to calculate diffusional limitations imposed by the stomata and the mesophyll. Together, they reduced the potential A_{net} by > 50% when conditions were otherwise optimal for photosynthesis and carboxylation capacity was at its peak (Fig. 6a). This seems counterintuitive, given that the highest g_s and g_m values occurred during this same period (Fig. 2b). However, this can be attributed to the shape of the CO₂-response curve, which is determined by the biochemical capacity (i.e. the demand for CO₂). A steeper initial slope in the summer yields a bigger limitation effect, compared with spring and autumn, when $V_{C_{max}}$ is lower, and so the initial slope of the response curve is relatively flat (Fig. 1b). On the flip side, this would suggest that reducing $V_{C_{max}}$ could reduce the relative diffusional limitations, but this would still come at a cost of reduced A_{net} at current ambient CO₂ concentrations. This trade-off between demand and supply highlights the need for a holistic approach for the improvement of photosynthesis through genetic manipulation (Flexas, 2016). Seasonally, diffusional limitations

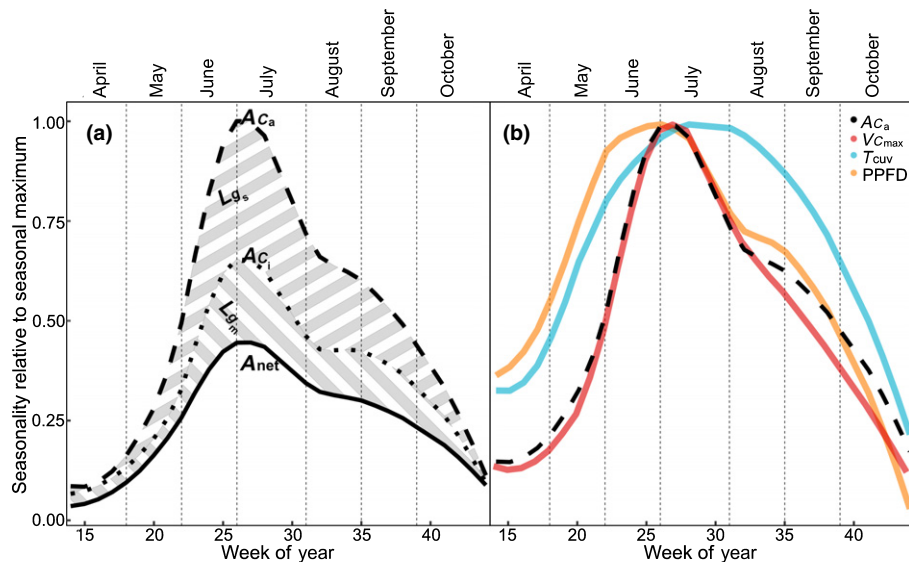


Fig. 6 Seasonality of photosynthesis and carboxylation capacity in *Pinus sylvestris*, and midday light and temperature conditions at the site, relative to their respective seasonal maximum. (a) The difference between the actual rate of photosynthesis (A_{net} , solid line) and the potential rates of photosynthesis without mesophyll limitation (A_{C_i} , dotted line) and without any diffusional limitation (A_{C_a} , dashed line) over the photosynthetic season. The difference between the lines represents the magnitude of mesophyll limitations (L_{g_m}) and stomatal limitations (L_{g_s}). (b) The seasonality of the temperature (T_{cuv} , light green) and light (PPFD, photosynthetic photon flux density; orange) conditions at the site, as well as the maximum carboxylation capacity ($V_{C_{\text{max}}}$, red). Note that the black dashed line on both figures is our estimate of $A_{C_a^*}$, the photosynthetic rate in the absence of diffusion limitations, normalized to its seasonal maximum.

reduced the potential rate of A_{net} to 25–50%, with L_{g_m} being relatively constant (19% on average), whereas L_{g_s} varied significantly over the course of the season (Figs 4, 6a), with a seasonal mean of 21%. This analysis also relied on the assumption of $V_{C_{\text{max}}}$ limitation. This assumption might not hold true for higher CO_2 concentrations, especially estimates at C_a , and would cause A_{C_a} , and consequently L_{g_s} , to be overestimated. Although this effect would be strongest on cold days, when L_{g_s} is low anyway and, therefore, would not strongly influence the seasonality of L_{g_s} . Furthermore, similar stomatal limitations were reported in Norway spruce (Wallin *et al.*, 1992), and similar mesophyll limitations were reported in hybrid poplar seedlings grown in a glasshouse (Xu *et al.*, 2019) and in soybean (Sun *et al.*, 2014). If the finding of seasonally constant L_{g_m} can be generalized across species, this could simplify the assumptions regarding nonstomatal limitations when optimality principles are applied in the modelling of stomatal behaviour (Dewar *et al.*, 2018; Gimeno *et al.*, 2019).

The seasonality of photosynthesis in northern conifers is tightly regulated by the seasonal fluctuations in temperature and light availability (Bergh *et al.*, 1998; Öquist & Hüner, 2003; Mäkelä *et al.*, 2004; Hall *et al.*, 2013; Stinziano *et al.*, 2015; Richardson *et al.*, 2018). During spring, photosynthetic capacity is heavily suppressed by nightly frost events (Ensminger *et al.*, 2004; Wallin *et al.*, 2013), and its subsequent recovery and acclimation are strongly coupled to temperature (Yang *et al.*, 2020). Therefore, the observed rates of A_{net} were low but consistently close to the potential rate of photosynthesis, as determined by $V_{C_{\text{max}}}$ (Fig. 6b), and L_T was close to zero (Fig. 5b). By contrast, in the autumn, $V_{C_{\text{max}}}$ remained relatively high (Figs 3, 6b) and, therefore, light-saturated A_{net} was suppressed primarily by daily

cold temperatures, seen as an increase of L_T late in the season (Fig. 5b). This conclusion differs from that of Kolari *et al.* (2014), who inferred, following the framework of Mäkelä *et al.* (2004), that the autumn decline in A_{net} was because of a reduction of $V_{C_{\text{max}}}$. In addition to L_T , A_{net} was often limited by low light (Fig. 5a,b) even during spring and summer, and L_{PPFD} further increased in the second half of the growing season as light-saturated conditions became less frequent (Fig. 5a,b).

Conclusions

Our analysis described for the first time the role of mesophyll conductance in connection with seasonal trends in net photosynthesis of *P. sylvestris*. Mesophyll conductance and A_{net} varied in tandem throughout the photosynthetic season, resulting in a nearly constant 19% mesophyll limitation. By contrast, stomatal conductance varied in a less coordinated fashion, resulting in seasonal shifts in the stomatal limitation and significant variation in the g_s/g_m ratio. We estimated $V_{C_{\text{max}}}$ using both intercellular CO_2 concentrations and chloroplast concentrations, finding that the two were significantly different only at the peak of the photosynthetic season. A parallel, empirical analysis of light and temperature limitations found short-term light and temperature effects superimposed on slow seasonal shifts in photosynthetic capacity. The short-term effects were most pronounced during the latter part of the season.

Acknowledgements

This work was supported by the Knut & Alice Wallenberg Foundation (#2015.0047) and the Swedish Strategic Research Area

BECC (Biodiversity and Ecosystem Services in a Changing Climate). We wish to acknowledge Jonas Lundholm at the SLU Stable Isotope Laboratory for the isotopic analysis of the calibration gases. We want to commemorate our colleague and dear friend Mats Råntfors, who has been vital in the set-up of the experiment and the maintenance of the gas-exchange system.

Author contributions

LT, GW, ZRS and JDM designed the experiment. ZRS performed the data analysis and wrote the manuscript, with LT, GW and JDM contributing to the interpretation of the results and providing editorial advice. All authors read and approved the final manuscript.

ORCID

John D. Marshall  <https://orcid.org/0000-0002-3841-8942>
Zsofia R. Stangl  <https://orcid.org/0000-0002-0119-747X>
Lasse Tarvainen  <https://orcid.org/0000-0003-3032-9440>
Göran Wallin  <https://orcid.org/0000-0002-5359-1102>

Data availability

The data presented here are available in Dataset S1. The raw data are available upon request to the authors.

References

- Bahar NHA, Hayes L, Scafaro AP, Atkin OK, Evans JR. 2018. Mesophyll conductance does not contribute to greater photosynthetic rate per unit nitrogen in temperate compared with tropical evergreen wet-forest tree leaves. *New Phytologist* 218: 492–505.
- Ball JT, Woodrow IE, Berry JA. 1987. A model predicting stomatal conductance and its contribution to the control of photosynthesis under different environmental conditions. In: Biggins J, ed. *Progress in photosynthesis research*. Dordrecht, the Netherlands: Martinus-Nijhoff Publishers, 221–224.
- Bauerle WL, Oren R, Way DA, Qian SS, Stoy PC, Thornton PE, Bowden JD, Hoffman FM, Reynolds RF. 2012. Photoperiodic regulation of the seasonal pattern of photosynthetic capacity and the implications for carbon cycling. *Proceedings of the National Academy of Sciences, USA* 29: 8612–8617.
- Bergh J, McMurtrie RE, Linder S. 1998. Climatic factors controlling the productivity of Norway spruce: a model-based analysis. *Forest Ecology and Management* 110: 127–139.
- Bernacchi CJ, Portis AR, Nakano H, von Caemmerer S, Long SP. 2002. Temperature response of mesophyll conductance. Implications for the determination of rubisco enzyme kinetics and for limitations to photosynthesis *in vivo*. *Plant Physiology* 130: 1992–1998.
- Bernacchi CJ, Singsaas EL, Pimentel C, Portis AR, Long SP. 2001. Improved temperature response functions for models of Rubisco-limited photosynthesis. *Plant, Cell & Environment* 24: 253–259.
- Burnett AC, Davidson KJ, Serbin SP, Rogers A. 2019. The ‘one-point method’ for estimating maximum carboxylation capacity of photosynthesis: a cautionary tale. *Plant, Cell & Environment* 42: 2472–2481.
- Busch FA, Holloway-Phillips M, Stuart-Williams H, Farquhar GD. 2020. Revisiting carbon isotope discrimination in C₃ plants shows respiration rules when photosynthesis is low. *Nature Plants* 6: 245–258.
- Busch FA, Sage RF. 2017. The sensitivity of photosynthesis to O₂ and CO₂ concentration identifies strong Rubisco control above the thermal optimum. *New Phytologist* 213: 1036–1051.
- von Caemmerer S, Farquhar GD. 1981. Some relationships between the biochemistry of photosynthesis and the gas exchange of leaves. *Planta* 153: 376–387.
- Cowan IR, Farquhar GD. 1977. Stomatal function in relation to leaf metabolism and environment. In: Jennings DH, ed. *Integration of activity in the higher plant*. Cambridge, UK: Cambridge University Press, 471–505.
- De Kauwe MG, Lin Y-S, Wright IJ, Medlyn BE, Crous KY, Ellsworth DS, Maire V, Prentice IC, Atkin OK, Rogers A *et al.* 2016. A test of the ‘one-point method’ for estimating maximum carboxylation capacity from field-measured, light-saturated photosynthesis. *New Phytologist* 210: 1130–1144.
- Dewar R, Mauranen A, Mäkelä A, Hölttä T, Medlyn B, Vesala T. 2018. New insights into the covariation of stomatal, mesophyll and hydraulic conductances from optimization models incorporating nonstomatal limitations to photosynthesis. *New Phytologist* 217: 571–585.
- Dusenge ME, Madhavji S, Way DA. 2020. Contrasting acclimation responses to elevated CO₂ and warming between an evergreen and a deciduous boreal conifer. *Global Change Biology* 26: 3639–3657.
- Ensminger I, Sveshnikov D, Campbell DA, Funk C, Jansson S, Lloyd J, Shibistova O, Öquist G. 2004. Intermittent low temperatures constrain spring recovery of photosynthesis in boreal Scots pine forests. *Global Change Biology* 10: 995–1008.
- Evans JR, von Caemmerer S. 2013. Temperature response of carbon isotope discrimination and mesophyll conductance in tobacco. *Plant, Cell & Environment* 36: 745–756.
- Farquhar GD, Cernusak LA. 2012. Ternary effects on the gas exchange of isotopologues of carbon dioxide. *Plant, Cell & Environment* 35: 1221–1231.
- Farquhar GD, Sharkey TD. 1982. Stomatal conductance and photosynthesis. *Annual Review of Plant Physiology* 33: 317–345.
- Farquhar GD, von Caemmerer S, Berry JA. 1980. A biochemical model of photosynthetic CO₂ assimilation in leaves of C₃ species. *Planta* 149: 78–90.
- Flexas J. 2016. Genetic improvement of leaf photosynthesis and intrinsic water use efficiency in C₃ plants: why so much little success? *Plant Science* 251: 155–161.
- Flexas J, Barbour MM, Brendel O, Cabrera HM, Carriqui M, Díaz-Espejo A, Douthe C, Dreyer E, Ferrio JP, Gago J *et al.* 2012. Mesophyll diffusion conductance to CO₂: an unappreciated central player in photosynthesis. *Plant Science* 193–194: 70–84.
- Flexas J, Niinemets U, Gallé A, Barbour MM, Centritto M, Díaz-Espejo A, Douthe C, Galmés J, Ribas-Carbo M, Rodriguez PL *et al.* 2013. Diffusional conductances to CO₂ as a target for increasing photosynthesis and photosynthetic water-use efficiency. *Photosynthesis Research* 117: 45–59.
- Flexas J, Ribas-Carbo M, Díaz-Espejo A, Galmés J, Medrano H. 2008. Mesophyll conductance to CO₂: current knowledge and future prospects. *Plant, Cell & Environment* 31: 602–621.
- Fracheboud Y, Luquez V, Björkén L, Sjödin A, Tuominen H, Jansson S. 2009. The control of autumn senescence in European aspen. *Plant Physiology* 149: 1982–1991.
- Gessler A, Tcherkez G, Peuke AD, Ghashghaie J, Farquhar GD. 2008. Experimental evidence for diel variations of the carbon isotope composition in leaf, stem and phloem sap organic matter in *Ricinus communis*. *Plant, Cell & Environment* 31: 941–953.
- Gimeno TE, Company CE, Drake JE, Barton CV, Tjoelker MG, Ubierna N, Marshall JD. 2021. Whole-tree mesophyll conductance reconciles isotopic and gas-exchange estimates of water-use efficiency. *New Phytologist* 229: 2535–2547.
- Gimeno TE, Saavedra N, Ogée J, Medlyn BE, Wingate L. 2019. A novel optimization approach incorporating non-stomatal limitations predicts stomatal behaviour in species from six plant functional types. *Journal of Experimental Botany* 70: 1639–1651.
- Grassi G, Magnani F. 2005. Stomatal, mesophyll conductance and biochemical limitations to photosynthesis as affected by drought and leaf ontogeny in ash and oak trees. *Plant, Cell & Environment* 28: 834–849.
- Hall M, Medlyn BE, Abramowitz G, Franklin O, Råntfors M, Linder S, Wallin G. 2013. Which are the most important parameters for modelling carbon assimilation in boreal Norway spruce under elevated [CO₂] and temperature conditions? *Tree Physiology* 33: 1156–1176.
- Hall M, Råntfors M, Slaney M, Linder S, Wallin G. 2009. Carbon dioxide exchange of buds and developing shoots of boreal Norway spruce exposed to

- elevated or ambient CO₂ concentration and temperature in whole-tree chambers. *Tree Physiology* 29: 461–481.
- Han Q, Kawasaki T, Nakano T, Chiba Y. 2004. Spatial and seasonal variability of temperature responses of biochemical photosynthesis parameters and leaf nitrogen content within a *Pinus densiflora* crown. *Tree Physiology* 24: 737–744.
- Hari P, Mäkelä A. 2003. Annual pattern of photosynthesis in Scots pine in the boreal zone. *Tree Physiology* 23: 145–155.
- Jach ME, Ceulemans R. 2000. Effects of season, needle age and elevated atmospheric CO₂ on photosynthesis in Scots pine (*Pinus sylvestris*). *Tree Physiology* 20: 145–157.
- Jensen AM, Warren JM, Hanson PJ, Childs J, Wullschlegel SD. 2015. Needle age and season influence photosynthetic temperature response and total annual carbon uptake in mature *Picea mariana* trees. *Annals of Botany* 116: 821–832.
- Jones HG. 1985. Partitioning stomatal and non-stomatal limitations to photosynthesis. *Plant, Cell & Environment* 8: 95–104.
- Katul GG, Palmroth S, Oren R. 2009. Leaf stomatal responses to vapour pressure deficit under current and CO₂-enriched atmosphere explained by the economics of gas exchange. *Plant, Cell & Environment* 32: 968–979.
- Knauer J, Zaehle S, De Kauwe MG, Haverd V, Reichstein M, Sun Y. 2020. Mesophyll conductance in land surface models: effects on photosynthesis and transpiration. *The Plant Journal* 101: 858–873.
- Kolari P, Chan T, Porcar-Castell A, Bäck J, Nikinmaa E, Juurola E. 2014. Field and controlled environment measurements show strong seasonal acclimation in photosynthesis and respiration potential in boreal Scots pine. *Frontiers in Plant Science* 5: e717.
- Kurepin LV, Stangl ZR, Ivanov AG, Bui V, Mema M, Hüner NPA, Öquist G, Way D, Hurrey V. 2018. Contrasting acclimation abilities of two dominant boreal conifers to elevated CO₂ and temperature. *Plant, Cell & Environment* 41: 1331–1345.
- Lamba S, Hall M, Rantfors M, Chaudhary N, Linder S, Way D, Uddling J, Wallin G. 2018. Physiological acclimation dampens initial effects of elevated temperature and atmospheric CO₂ concentration in mature boreal Norway spruce. *Plant, Cell & Environment* 41: 300–313.
- Leuning R. 1995. A critical appraisal of a coupled stomatal–photosynthesis model for C₃ plants. *Plant, Cell & Environment* 18: 339–357.
- Lim H, Oren R, Palmroth S, Tor-ngern P, Mörling T, Näsholm T, Lundmark T, Helmissaari H-S, Leppälampi-Kujansuu J, Linder S. 2015. Inter-annual variability of precipitation constrains the production response of boreal *Pinus sylvestris* to nitrogen fertilization. *Forest Ecology and Management* 348: 31–45.
- Ma WT, Tcherkez G, Wang XM, Schäufele R, Schnyder H, Yang Y, Gong XY. 2021. Accounting for mesophyll conductance substantially improves ¹³C-based estimates of intrinsic water-use efficiency. *New Phytologist* 229: 1326–1338.
- Mäkelä A, Hari P, Berninger F, Hänninen H, Nikinmaa E. 2004. Acclimation of photosynthetic capacity in Scots pine to the annual cycle of temperature. *Tree Physiology* 24: 369–376.
- Marshall B, Bischoff PV. 1980. A model for C₃ leaves describing the dependence of net photosynthesis on irradiance: II. Application to the analysis of flag leaf photosynthesis. *Journal of Experimental Botany* 31: 41–48.
- Medlyn BE, Dreyer E, Ellsworth D, Forstreuter M, Harley PC, Kirschbaum MUF, Le Roux X, Montpied P, Strassmeyer J, Walcroft A *et al.* 2002a. Temperature response of parameters of a biochemically based model of photosynthesis. II. A review of experimental data. *Plant, Cell & Environment* 25: 1167–1179.
- Medlyn BE, Duursma RA, Eamus D, Ellsworth DS, Prentice IC, Barton CVM, Crous KY, De Angelis P, Freeman M, Wingate L. 2011. Reconciling the optimal and empirical approaches to modelling stomatal conductance. *Global Change Biology* 17: 2134–2144.
- Medlyn BE, Loustau D, Delzon S. 2002b. Temperature response of parameters of a biochemically based model of photosynthesis. I. Seasonal changes in mature maritime pine (*Pinus pinaster* Ait.): seasonal changes in temperature response of photosynthetic parameters. *Plant, Cell & Environment* 25: 1155–1165.
- Miyazawa Y, Kikuzawa K. 2006. Physiological basis of seasonal trend in leaf photosynthesis of five evergreen broad-leaved species in a temperate deciduous forest. *Tree Physiology* 26: 249–256.
- Öquist G, Hüner NPA. 2003. Photosynthesis of overwintering evergreen plants. *Annual Review of Plant Biology* 54: 329–355.
- Pons TL, Flexas J, von Caemmerer S, Evans JR, Genty B, Ribas-Carbo M, Bruynoli E. 2009. Estimating mesophyll conductance to CO₂: methodology, potential errors, and recommendations. *Journal of Experimental Botany* 60: 2217–2234.
- Richardson AD, Hufkens K, Milliman T, Aubrecht DM, Furze ME, Seyedinrollah B, Krassovski MB, Latimer JM, Nettles WR, Heiderman RR *et al.* 2018. Ecosystem warming extends vegetation activity but heightens vulnerability to cold temperatures. *Nature* 560: 368–371.
- Rogers A, Medlyn BE, Dukes JS, Bonan G, von Caemmerer S, Dietze MC, Kattge J, Leakey ADB, Mercado LM, Niinemets Ü *et al.* 2017. A roadmap for improving the representation of photosynthesis in Earth system models. *New Phytologist* 213: 22–42.
- Sage RF, Kubien DS. 2007. The temperature response of C₃ and C₄ photosynthesis. *Plant, Cell & Environment* 30: 1086–1106.
- Sage RF, Way DA, Kubien DS. 2008. Rubisco, Rubisco activase, and global climate change. *Journal of Experimental Botany* 59: 1581–1595.
- Schiestl-Aalto P, Stangl ZR, Tarvainen L, Wallin G, Marshall J, Mäkelä A. 2021. Linking canopy-scale mesophyll conductance and phloem sugar δ¹³C using empirical and modelling approaches. *New Phytologist* 229: 3141–3155.
- Sharkey TD. 1985. O₂-insensitive photosynthesis in C₃ plants. Its occurrence and a possible explanation. *Plant Physiology* 78: 71–75.
- Stangl ZR, Tarvainen L, Wallin G, Ubierna N, Rantfors M, Marshall JD. 2019. Diurnal variation in mesophyll conductance and its influence on modelled water-use efficiency in a mature boreal *Pinus sylvestris* stand. *Photosynthesis Research* 141: 53–63.
- Stinziano JR, Hüner NPA, Way DA. 2015. Warming delays autumn declines in photosynthetic capacity in a boreal conifer, Norway spruce (*Picea abies*). *Tree Physiology* 35: 1303–1313.
- Sun J, Feng Z, Leakey ADB, Zhu X, Bernacchi CJ, Ort DR. 2014. Inconsistency of mesophyll conductance estimate causes the inconsistency for the estimates of maximum rate of Rubisco carboxylation among the linear, rectangular and non-rectangular hyperbola biochemical models of leaf photosynthesis – a case study of CO₂ enrichment and leaf aging effects in soybean. *Plant Science* 226: 49–60.
- Sun Y, Gu L, Dickinson RE, Norby RJ, Pallardy SG, Hoffman FM. 2014a. Impact of mesophyll diffusion on estimated global land CO₂ fertilization. *Proceedings of the National Academy of Sciences, USA* 111: 15774–15779.
- Sun Y, Gu L, Dickinson RE, Pallardy SG, Baker J, Cao Y, Damatta FM, Dong X, Ellsworth D, Van Goethem D *et al.* 2014b. Asymmetrical effects of mesophyll conductance on fundamental photosynthetic parameters and their relationships estimated from leaf gas exchange measurements. *Plant, Cell & Environment* 37: 978–994.
- Tarvainen L, Lutz M, Rantfors M, Näsholm T, Wallin G. 2016. Increased needle nitrogen contents did not improve shoot photosynthetic performance of mature nitrogen-poor Scots pine trees. *Frontiers in Plant Science* 7: e1051.
- Tarvainen L, Lutz M, Rantfors M, Näsholm T, Wallin G. 2018. Temperature responses of photosynthetic capacity parameters were not affected by foliar nitrogen content in mature *Pinus sylvestris*. *Physiologia Plantarum* 162: 370–378.
- Tarvainen L, Rantfors M, Wallin G. 2015. Seasonal and within-canopy variation in shoot-scale resource use efficiency trade-offs in a Norway spruce stand. *Plant, Cell & Environment* 38: 2487–2496.
- Tian X, Minunno F, Schiestl-Aalto P, Chi J, Zhao P, Peichl M, Marshall JD, Näsholm T, Lim H, Peltoniemi P *et al.* 2021. Disaggregating the effects of nitrogen addition on gross primary production in a boreal Scots pine forest. *Agricultural and Forest Meteorology* 108337: 301–302.
- Troeng E, Linder S. 1982. Gas exchange in a 20-year-old stand of Scots pine. *Physiologia Plantarum* 54: 15–23.
- Uddling J, Wallin G. 2012. Interacting effects of elevated CO₂ and weather variability on photosynthesis of mature boreal Norway spruce agree with biochemical model predictions. *Tree Physiology* 32: 1509–1521.
- Wallin G, Hall M, Slaney M, Rantfors M, Medhurst J, Linder S. 2013. Spring photosynthetic recovery of boreal Norway spruce under conditions of elevated [CO₂] and air temperature. *Tree Physiology* 33: 1177–1191.
- Wallin G, Linder S, Lindroth A, Rantfors M, Flemberg S, Grelle A. 2001. Carbon dioxide exchange in Norway spruce at the shoot, tree and ecosystem scale. *Tree Physiology* 21: 969–976.

- Wallin G, Ottosson S, Selldén G. 1992. Long term exposure of Norway spruce, *Picea abies* (L.) Karst., to ozone in open-top chambers. IV. Effects on the stomatal and the non-stomatal limitation of photosynthesis and on the carboxylation efficiency. *New Phytologist* 121: 395–401.
- Warren CR. 2008. Stand aside stomata, another actor deserves centre stage: the forgotten role of the internal conductance to CO₂ transfer. *Journal of Experimental Botany* 59: 1475–1487.
- Way DA, Yamori W. 2014. Thermal acclimation of photosynthesis: on the importance of adjusting our definitions and accounting for thermal acclimation of respiration. *Photosynthesis Research* 119: 89–100.
- Wilson KB, Baldocchi DD, Hanson PJ. 2000. Spatial and seasonal variability of photosynthetic parameters and their relationship to leaf nitrogen in a deciduous forest. *Tree Physiology* 20: 565–578.
- Wingate L, Seibt U, Moncrieff JB, Jarvis PG, Lloyd J. 2007. Variations in ¹³C discrimination during CO₂ exchange by *Picea sitchensis* branches in the field. *Plant, Cell & Environment* 30: 600–616.
- Xu Y, Feng Z, Shang B, Dai L, Uddling J, Tarvainen L. 2019. Mesophyll conductance limitation of photosynthesis in poplar under elevated ozone. *Science of the Total Environment* 657: 136–145.
- Xu Y, Shang B, Feng Z, Tarvainen L. 2020. Effect of elevated ozone, nitrogen availability and mesophyll conductance on the temperature responses of leaf photosynthetic parameters in poplar. *Tree Physiology* 40: 484–497.
- Yang Q, Blanco NE, Hermida-Carrera C, Lehotai N, Hurry V, Strand Å. 2020. Two dominant boreal conifers use contrasting mechanisms to reactivate photosynthesis in the spring. *Nature Communications* 11: e128.

Supporting Information

Additional Supporting Information may be found online in the Supporting Information section at the end of the article.

Dataset S1 Seasonal mid-day data of light and temperature conditions, and gas-exchange parameters of upper-canopy shoots of mature *Pinus sylvestris*.

Fig. S1 Examples of fitted photosynthetic light-response models.

Fig. S2 Temperature response of net photosynthesis during different periods of the season.

Fig. S3 Illustration of the optimum temperature ranges over the season.

Fig. S4 Temperature responses of $V_{C_{max}}(C_i)$ and $V_{C_{max}}(C_c)$.

Fig. S5 Seasonality of mean mid-day g_s/g_m ratio under saturating light conditions.

Fig. S6 Seasonal $V_{C_{max}}(C_i)$ plotted against $V_{C_{max}}(C_c)$.

Methods S1 Estimation of day-time respiration over the season.

Methods S2 Estimation of ¹³C discrimination.

Please note: Wiley Blackwell are not responsible for the content or functionality of any Supporting Information supplied by the authors. Any queries (other than missing material) should be directed to the *New Phytologist* Central Office.